

Accepted Manuscript

Designed P-glycoprotein inhibitors with triazol-tetrahydroisoquinoline-core increase doxorubicin-induced mortality in multidrug resistant K562/A02 cells

Mutta Kairuki, Qianqian Qiu, Miaobo Pan, Qifei Li, Jiaqi Zhou, Hesham Ghaleb, Wenlong Huang, Hai Qian, Cheng Jiang

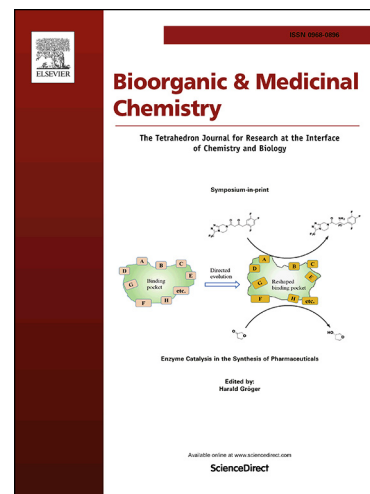
PII: S0968-0896(19)30775-8
DOI: <https://doi.org/10.1016/j.bmc.2019.06.013>
Reference: BMC 14950

To appear in: *Bioorganic & Medicinal Chemistry*

Received Date: 9 May 2019
Revised Date: 4 June 2019
Accepted Date: 6 June 2019

Please cite this article as: Kairuki, M., Qiu, Q., Pan, M., Li, Q., Zhou, J., Ghaleb, H., Huang, W., Qian, H., Jiang, C., Designed P-glycoprotein inhibitors with triazol-tetrahydroisoquinoline-core increase doxorubicin-induced mortality in multidrug resistant K562/A02 cells, *Bioorganic & Medicinal Chemistry* (2019), doi: <https://doi.org/10.1016/j.bmc.2019.06.013>

This is a PDF file of an unedited manuscript that has been accepted for publication. As a service to our customers we are providing this early version of the manuscript. The manuscript will undergo copyediting, typesetting, and review of the resulting proof before it is published in its final form. Please note that during the production process errors may be discovered which could affect the content, and all legal disclaimers that apply to the journal pertain.



Designed P-glycoprotein inhibitors with triazol-tetrahydroisoquinoline-core increase doxorubicin-induced mortality in multidrug resistant K562/A02 cells

Mutta Kairuki ^{1,#}, Qianqian Qiu ^{2,#}, Miaobo Pan¹, Qifei Li¹, Jiaqi Zhou¹, Hesham Ghaleb¹, Wenlong Huang^{1,3}, Hai Qian^{1,3,*} and Cheng Jiang^{4,*}

¹ Center of Drug Discovery, State Key Laboratory of Natural Medicines, China Pharmaceutical University, 24 Tongjiaxiang, Nanjing 210009, PR China

² School of Pharmacy, Jiangsu Provincial Key Laboratory of Coastal Wetland Bioresources and Environmental Protection, Yancheng Teachers' University, Yancheng, PR China

³ Jiangsu Key Laboratory of Drug Discovery for Metabolic Disease, China Pharmaceutical University, 24 Tongjiaxiang, Nanjing 210009, PR China

⁴ Department of Medicinal Chemistry, China Pharmaceutical University, Nanjing 210009, PR China

Mutta Kairuki and Qianqian Qiu contributed equally as first authors.

*Co-corresponding authors: Hai Qian, Jiangsu Key Laboratory of Drug Discovery for Metabolic Disease, China Pharmaceutical University, 24 Tongjiaxiang, Nanjing 210009, PR China. Phone, +86-25-83271051; Fax, +86-25-83271051; E-mail, qianhai24@163.com.

Cheng Jiang, Department of Medicinal chemistry, China Pharmaceutical University, Nanjing 210009, PR China Phone, +86-25-83271051; Fax, +86-25-83271051; E-mail, jc@cpu.edu.cn

Abstract

Multidrug resistance (MDR) refers to the cross-resistance of cancer cells to one drug, accompanied by other drugs with different mechanisms and structures, which is one of the main obstacles of clinical chemotherapy. Overexpression of P-glycoprotein (P-gp) was an extensively studied cause of MDR. Therefore, inhibiting P-gp have become an important strategy to reverse MDR. In this study, two series of triazole-tetrahydroisoquinoline-core P-gp inhibitors were designed and synthesized. Among them, compound **I-5** had a remarkable reversal activity of MDR activity and the preliminary mechanism study was also carried out. All the results proved that compound **I-5** was considered as a promising P-gp-mediated MDR reversal candidate.

Keywords: Multidrug resistance; P-glycoprotein; reversal activity; K562/A02 cells

1. Introduction

Malignant cancer is one of the diseases that seriously threaten human survival.[1] Chemotherapy is one of the main treatments for cancer. With the development of chemotherapeutics, the mortality rate of cancer patients was declined significantly, but the resistance of cancer cells to chemotherapeutics hinders the cure of clinical malignant tumors, and greatly increases the recurrence and mortality of cancer[2, 3]. Multidrug resistance is the most serious one. Multidrug resistance (MDR) refers to the cross-resistance of cancer cells to one drug, accompanied by other drugs with different mechanisms and structures. The mechanisms of MDR have been extensively studied [4-7]. Among these mechanisms, overexpression of ATP-binding cassette subfamily (ABC) transmembrane transporter was the most significant one, which enhances the translocation of cytotoxic drugs and results in the reduction of intracellular drug concentration lower than the effective concentration[8, 9]. P-glycoprotein (P-gp) is encoded by MDR1 gene, consisting of 1280 amino acids. It is one of the most thoroughly studied ABC transporter families[10]. As a key protein regulating multidrug resistance in many kinds of cancer cells, overexpression of P-gp results in the concentration of antineoplastic drugs in tumor cells lower than the

effective concentration, making loss of cytotoxicity or apoptotic activity. Therefore, inhibiting the function of P-gp and reducing the efflux of anti-cancer drugs have become an important strategy to reverse MDR [11, 12].

Verapamil (VRP), a calcium antagonist, was firstly discovered to have the power of reversing MDR in cancer cells by Tsuruo et al. in 1981[13]. In the past forty years, many P-gp inhibitors with different structures and mechanisms have been found, some of which have entered the stage of clinical research [14-17]. However, an ABCB1 inhibitor has not been approved for the market due to a lack of significant clinical efficacy, pharmacokinetic interaction, or concerns about its safety [14]. As a result, developing novel, targeted, and potent ABCB1 inhibitors to reverse drug resistance is in a great need.

It has been reported that the tetrahydroisoquinolinethylphenylamine-based P-gp inhibitors showed potent MDR reversal activity, including WK-X-34, Tariquidar (Tar) and HM30181[18-21]. In addition, triazole, as a crucial nitrogen-heterocycle, also attracted our attention due to its wide application as ABCB1 inhibitors to reverse MDR, as well as its easy accessibility. 1,2,3-triazole has the similar bond length and plane structure with amide bond, which can play better π - π interaction with receptor proteins [22]. Heterocycles such as indole, quinoline, thiophene and furan ring play an important role in anti-cancer drugs. From the above, we designed series I compounds as shown in **Fig.1A**. In order to reduce molecular weight and improve the druggability, the designed structures were in further simplification to get series II compounds. As the docking results shown in **Fig.1B**, one of the typical designed structure of series I (**I-1**) and series II (**II-1**) both occupied hydrophobic pocket of P-gp protein (PDB ID:6FN1) in a similar interaction mode. I-1 has Pi-Pi stacking action with PHE982 and PHE302, and forms hydrogen-bond interaction with GIN945. Similarly, II-1 has PI-PI stacking interaction with PHE982 and hydrogen-bond with TYR952. Hence, it is believed that the two series of compounds may have similar activities. Consequently, 24 novel tetrahydroisoquinoline P-gp inhibitors were synthesized and founded that some of them exhibited a powerful improvement of reversal activity.

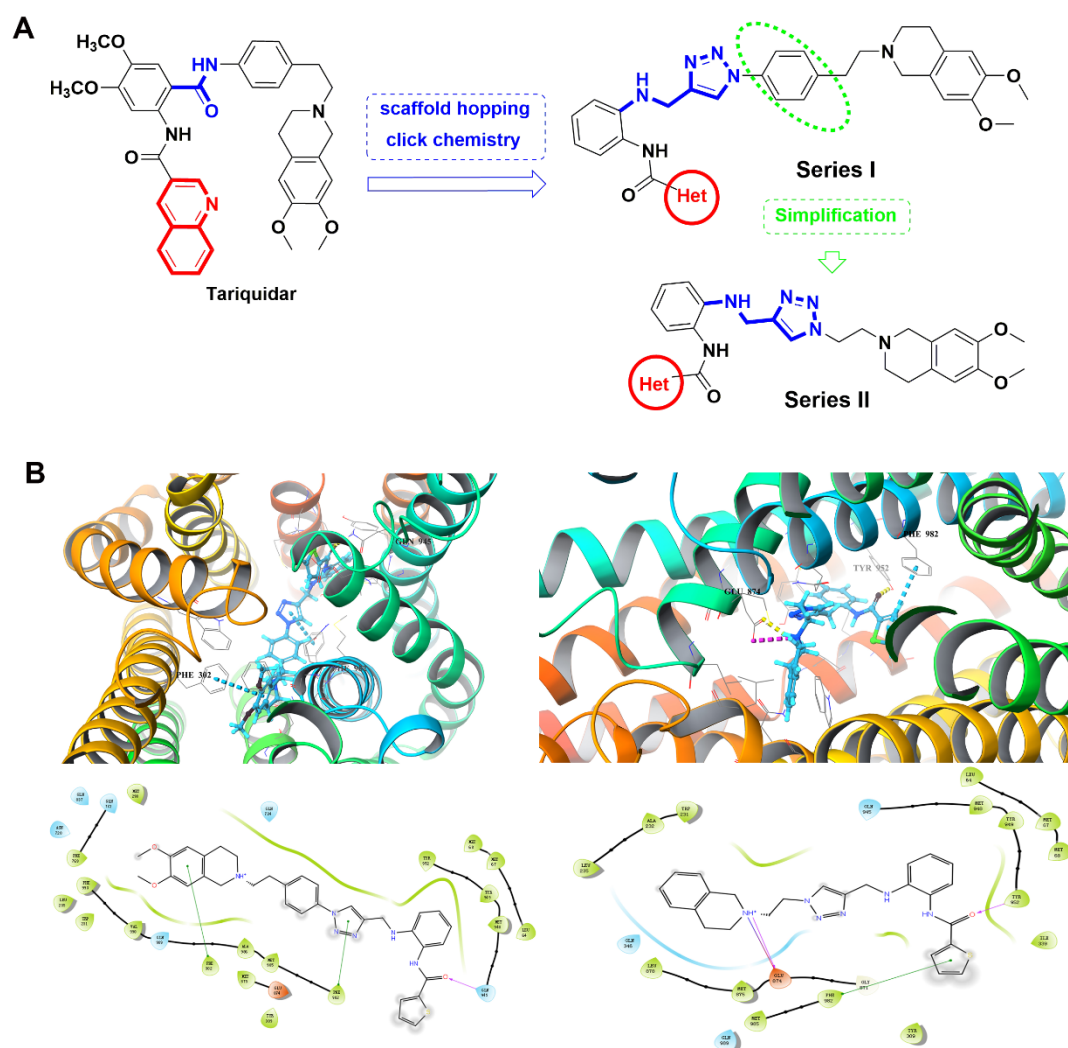


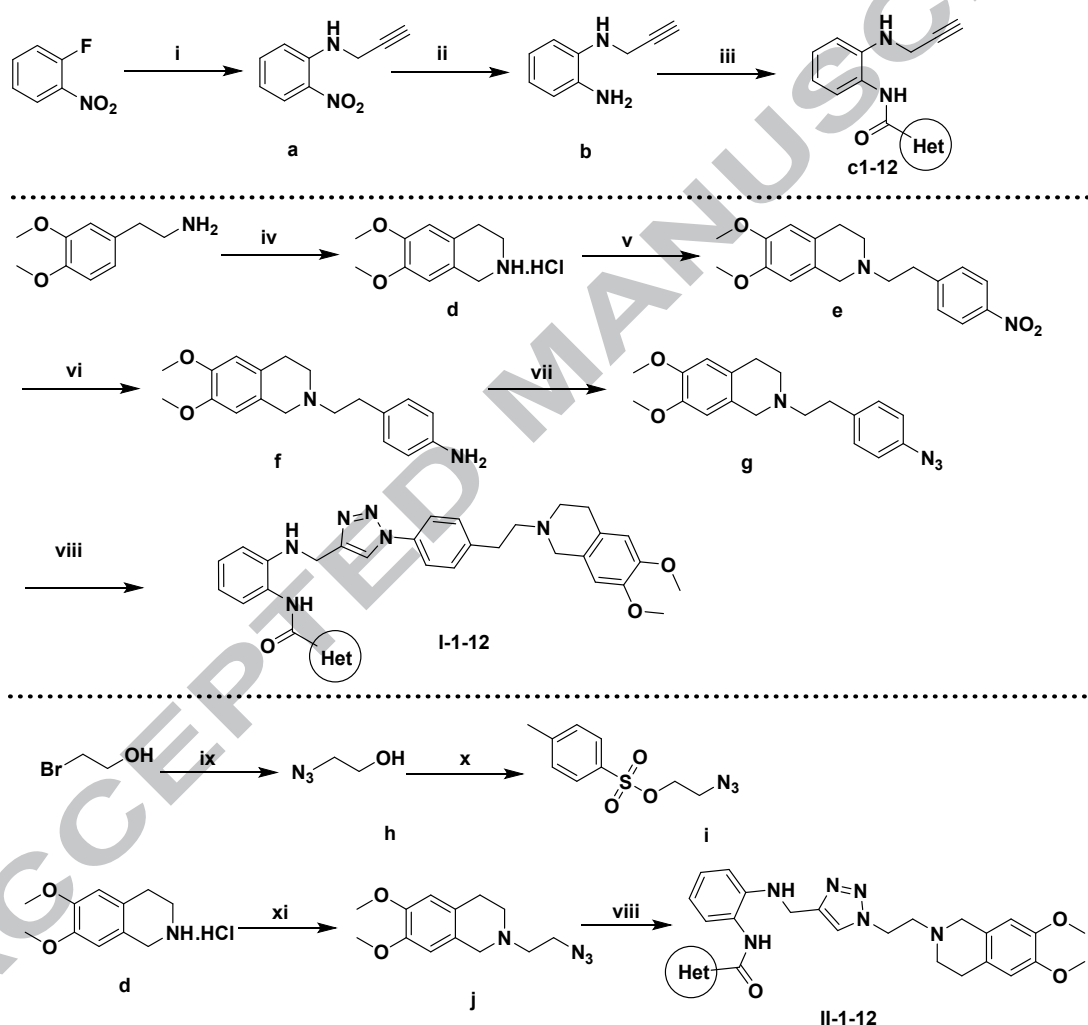
Figure 1. (A) Design of the target compounds; (B) Structure docking results with P-gp (PDB ID:6FN1).

2. Results and discussion

2.1 chemistry

As depicted in scheme 1, the two series compounds **I-1-12** and **II-1-12** with triazol-tetrahydroisoquinoline-core were synthesized. Compound **a** was prepared from the starting material 1-fluoro-2-nitrobenzene refluxed in the mixture of DMF with prop-2-yn-1-amine and potassium carbonate for 8h.[23] Treatment of compound **a** with sodium hyposulfite in 50% ethanol afforded compound **b** which was then reacted with disparate aromatic formic acid in dry dichloromethane with 1-(3-dimethylaminopropyl)-3-ethylcarbodiimide hydrochloride (EDCI), 1-Hydroxybenzotriazole (HOBT) as coupling agents to get the compound **c1-12** [24].

Compounds **g** and **j** were synthesized according to literature procedures with minor modification [25, 26]. Subsequently, compound **g** or **j** and compounds **c1-12** were treated with ascorbate sodium and copper sulfate in 75% methanol stirring at room temperature for 48 h to provide compounds **I-1-12** and **II-1-12**. Most of the target compounds could be precipitated from the reaction solution directly, for higher purity they should be purified by column chromatography. The structures of target compounds obtained were listed in **Table 1**.

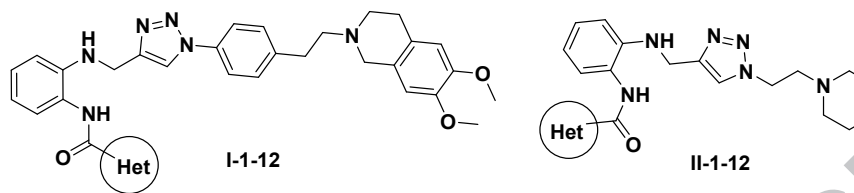


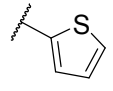
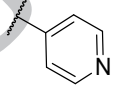
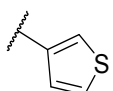
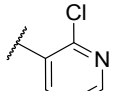
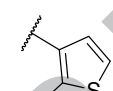
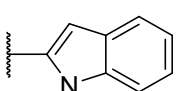
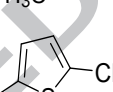
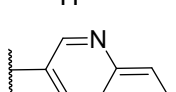
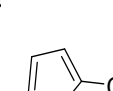
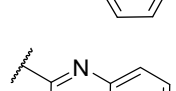
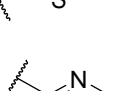
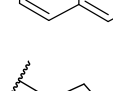
Scheme 1. Synthesis of the target compounds.

Reagents and conditions: (i) 2-Propynylamine, K_2CO_3 , DMF, $80^\circ C$, 8h; (ii) $Na_2S_2O_4$, $NaHCO_3$, MeOH: H_2O : THF=1:1:1, $0^\circ C \sim r.t.$, 12 h; (iii) EDCI, HOBT $r.t.$, 24 h; (iv) $(CH_2O)_n$, EtOH, $r.t.$, 3h; con. HCl, reflux, 4h; (v) 1-(2-bromoethyl)-4-nitrobenzene, K_2CO_3 , CH_3CN , reflux, 17h; (vi) $H_2/Pd-C$, DCM/EtOH, $r.t.$, 24h; (vii) $NaNO_2$, 50% AcOH, $0^\circ C \sim 5^\circ C$, 30 min; NaN_3 , $0^\circ C \sim 5^\circ C$, 50 min; (viii) **c1-12**, sodium ascorbate,

CuSO₄, 75% CH₃OH, 24h~48h; (ix) NaN₃, H₂O, 80 °C, 24 h; (x) TEA/DCM, TsCl, r.t., 24 h; (xi) **i**, TEA, acetonitrile, 60 °C.

Table 1. Structures of Target Compounds



Compound	Het	Compound	Het
I-1 / II-1		I-7 / II-7	
I-2 / II-2		I-8 / II-8	
I-3 / II-3		I-9 / II-9	
I-4 / II-4		I-10 / II-10	
I-5 / II-5		I-11 / II-11	
I-6 / II-6		I-12 / II-12	

2.2 Cytotoxicity evaluation

Due to toxicity at the therapeutic concentration range, the majority of potent P-gp inhibitors are failed for further studies, the intrinsic cytotoxicity of target compounds against parental human erythroleukemia sensitive cell line K562 and its doxorubicin (DOX)-selected derivative P-gp overexpressing K562/A02 cells was evaluated by MTT assay. As shown in **Table 2**, the anticarcinogen DOX exhibited weak inhibitory effect on the survival of K562/A02 cells (IC₅₀ of 55.47 ± 1.67 μM), which was about 108.8-fold greater resistance than K562 cells (IC₅₀ = 0.51 ± 0.09 μM). Except the potent inhibitor Tariquidar (18.42 ± 1.12 μM for K562 cells and 30.10 ± 2.16 μM for

K562/A02 cells), most of the 24 target compounds had low intrinsic cytotoxicity ($IC_{50} > 40 \mu\text{M}$) against both K562 and K562/A02 cells. It can be seen from data points of IC_{50} that the survival rates of all compounds at $5.0 \mu\text{M}$ were all over 95%, appropriate to determine its reversal effect on K562/A02 cells. Therefore, the reversal activity of **I-1-12** and **II-1-12** in DOX-resistance were determined preliminarily at non-toxic concentration of $5.0 \mu\text{M}$ by MTT.

Table 2. Cytotoxicity of the target compounds on K562 and K562/A02 cells^a.

Cpd.	$IC_{50}(\mu\text{M})$		Cpd.	$IC_{50}(\mu\text{M})$	
	K562	K562/A02		K562	K562/A02
I-1	>100	60.71 ± 2.3	II-1	>100	>100
I-2	>100	65.93 ± 4.3	II-2	>100	>100
I-3	>100	59.55 ± 1.9	II-3	>100	>100
I-4	>100	>100	II-4	>100	>100
I-5	>100	63.23 ± 2.3	II-5	57.88 ± 0.56	>100
I-6	45.09 ± 1.2	52.08 ± 1.5	II-6	>100	>100
I-7	>100	>100	II-7	>100	>100
I-8	42.7 ± 1.33	46.99 ± 0.92	II-8	>100	>100
I-9	>100	>100	II-9	>100	>100
I-10	>100	>100	II-10	>100	>100
I-11	>100	58.13±2.4	II-11	>100	43.71 ± 1.34
I-12	25.76 ± 0.92	58.39±1.9	II-12	>100	>100
VRP	68.27 ± 3.54	59.24 ± 3.12	Tar	18.42 ± 1.12	30.10 ± 2.16
DOX	0.51 ± 0.09	55.47 ± 1.67			

^a Cytotoxicity of target compounds toward cells were determined by MTT assay and data are presented as mean ± SD for three independent tests.

2.3 P-gp modulating activity of the target compounds on reversing DOX resistance in K562/A02 cells and structure-activity relationships

Based on the results above, all the target compounds were investigated for further reversal activity at $5.0 \mu\text{M}$ with verapamil (VRP) and Tariquidar (Tar) as positive controls. As the results summarized in **Table 3**, the combination of most target compounds enhanced the toxic effect of DOX in K562/A02 cells. P-gp modulating activity of compounds was evaluated by a parameter known as reversal fold (RF).

Most of the target compounds showed much more active MDR reversal activity than **VRP** at the same concentration. Especially, compound **I-5** exerted the strongest reversal activity with RF of 42, which similar to Tar (RF = 42.3).

According to **Table 3**, the activities of series I compounds with the triazole-N-phenylethyl tetrahydroisoquinoline moiety were much better than that of simplified series II compounds. It was speculated that the simplification of the benzene ring structure reduced the hydrophobicity of the compounds and thus affected the reversal activity. For the docking results in **Fig.1B**, the most difference between the two compounds is that the benzene ring of tetrahydroisoquinoline in **I-1** can have Pi-Pi stacking with PHE302, while **II-1** loses its interaction with PHE302 because of shortening the length of the whole molecule. However, tertiary amine N atom of **II-1** could capture hydrogen ion, forming positive charge center, to interact with residue GLU874. Based on the determined results in reversal activity, it is concluded that the molecular structure contributes more to the P-gp active conformation through PHE302, which directly affects the final reversal activity. Besides, in series I compounds, several thiophene ring derivatives exhibited prominent activity, presumably because the introduction of sulfur atoms in heterocycles can change the charge distribution of compounds and increase the hydrophobicity of compounds. In addition, the introduction of chlorine atoms can further increase lipophilicity, enhance its affinity with binding sites of P-gp hydrophobic cavity, and improve the metabolic instability of thiophene rings. Therefore, the compound **I-5** showed the strongest reversal activity.

Table 3. DOX-resistance reversal activity of target compounds at 5.0 μM concentration in K562/A02 cells ^a.

Compound (5.0 μM)	IC ₅₀ /DOX (μM)	RF	Compound (5.0 μM)	IC ₅₀ /DOX (μM)	RF
I-1	2.62 \pm 0.3	21.17	II-1	27.30 \pm 0.23	2.03
I-2	2.43 \pm 0.35	22.82	II-2	24.37 \pm 0.89	2.27
I-3	5.10 \pm 0.21	10.87	II-3	17.90 \pm 0.33	3.09

I-4	2.54 ± 0.19	21.83	II-4	19.37 ± 0.78	2.86
I-5	1.32 ± 0.07	42.02	II-5	14.37 ± 1.27	3.38
I-6	4.69 ± 0.32	11.83	II-6	14.29 ± 1.82	3.88
I-7	51.06 ± 2.3	1.09	II-7	14.81 ± 2.38	3.74
I-8	19.88 ± 1.2	2.79	II-8	43.26 ± 5.43	1.28
I-9	8.44 ± 1.11	6.57	II-9	13.32 ± 2.09	4.16
I-10	14.52 ± 0.92	3.82	II-10	29.57 ± 2.33	1.88
I-11	4.17 ± 0.89	13.30	II-11	4.11 ± 0.45	13.5
I-12	4.93 ± 0.23	11.25	II-12	43.46 ± 5.65	1.28
VRP	7.084 ± 0.67	7.83	DOX	55.47 ± 1.67	1.00
Tar	1.33 ± 0.22	42.34			

^a The IC₅₀ value was determined after exposure to a series of DOX concentration with different target compounds at 1.0 μM using K562/A02 cells; Reversal fold (RF, fold-change in drug sensitivity) = (IC₅₀ without inhibitor / (IC₅₀ with inhibitor). Data were analyzed with GraphPad Prism 5.0 software and presented as mean ± SD for three independent tests.

2.4 Chemo-sensitizing effect of target compound

Based on the reversal activity, compound **I-5** was considered as the most promising candidate for further dose-response reversal effect at different concentrations (5.0 μM, 2.0 μM, 1.0 μM, 0.5 μM, 0.25 μM, 0.1 μM, 0.075 μM, 0.05 μM, 0.025 μM, 0.01 μM and 0.005 μM) towards K562/A02 cells. As shown in Figure 2, there was still weak reversal activity of **I-5** even at 10 nM and the EC₅₀ value of **I-5** was only (46.83 ± 4.6) nM calculated by the doseresponse curve in GraphPad Prism 7.0 software, indicating **I-5** was so powerful in inverting DOX resistance.

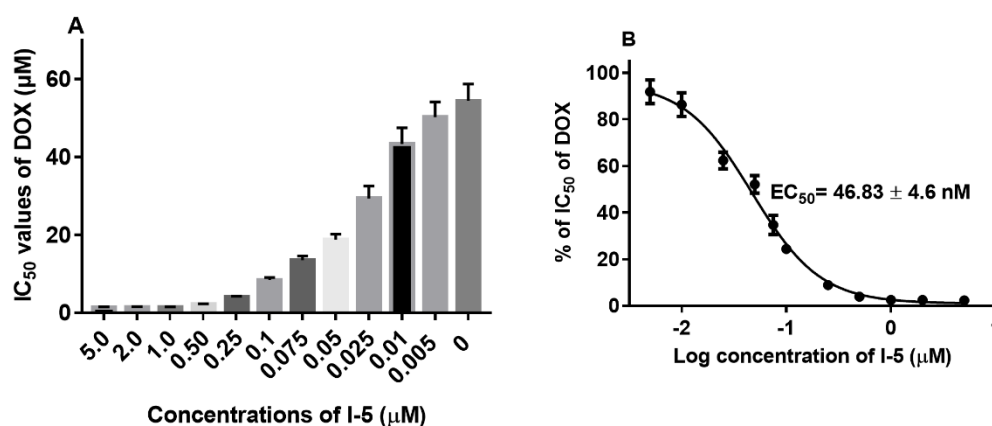


Figure 2. Impact of **I-5** on inverting DOX resistance in K562/A02 cells. (A) IC₅₀ values of DOX in K562/A02 cells dealt with DOX with/without different concentrations of **I-5**; (B) EC₅₀ value for **I-5** in depressing DOX-resistance of K562/A02 cells. The percentage of DOX IC₅₀ was charted with log concentration of **I-5**, which is equal to (DOX IC₅₀ in each modulator concentration/DOX IC₅₀ without modulator) × 100%. Thus, EC₅₀ can be noted for the modulator concentration, which can diminish the DOX IC₅₀ by 50%.

2.5 Duration of reversal effects

The relatively long duration of reversal action is a required condition for P-gp inhibitors. To further ensure the combination of **I-5** and anti-cancer drugs could exert great activity, the duration of reversal effect of **I-5** was determined. As the results shown Table 4, the duration of reversal effects for both compound 3 and positive tariquidar at a concentration of 5 µM were over 24 h resulting in a significantly longer duration of action than VRP with the same concentration.

Table 4. Duration of MDR reversal effect in K562/A02 cells after incubation and washout of **I-5**.

Treatment schedule	IC ₅₀ of DOX(µM) (RF) ^a			
	Control	VRP (5 µM)	Tar (5 µM)	I-5 (5 µM)
No wash	55.47 ± 1.67 (1.00)	7.08 ± 0.67 (7.83)	1.33 ± 0.22 (42.34)	1.32 ± 0.07 (42.02)
Wash, 0h	ND ^b	26.24 ± 2.68 (2.11)	2.89 ± 0.34 (19.19)	3.26 ± 0.91 (17.05)

Wash, 6h	ND	>50	5.13 ± 0.54 (10.18)	7.84 ± 0.68 (7.08)
Wash, 12h	ND	ND	13.45 ± 1.22 (4.12)	16.84 ± 1.68 (3.29)
Wash, 24h	ND	ND	23.14 ± 2.14 (2.40)	33.47 ± 2.63 (1.27)

^a Reversal fold (RF) = (IC₅₀ without inhibitor)/(IC₅₀ with inhibitor). The values were presented as the mean ± SD for three independent tests. ^b ND: not determined.

2.6 Effect of target compound on P-gp function

2.6.1 DOX accumulation

Furthermore, to validate our assumption that whether the reversal effect of compound **I-5** is associated with a concomitant increase in DOX accumulation, we utilized fluorescence microscope to give a further evaluation.[27] As shown in **Figure 3A**, sensitive K562 cells retained most of the red fluorescence after incubation. While it was almost dark in K562/A02 cells, for the overexpressed P-gp had pumped most of the DOX out of the cells. It was encouraging to find that incubation with compound **I-5** could induce more DOX accumulation than VRP at the same condition.

When incubated with modulators at various concentrations, the fluorescence intensity of DOX accumulated in K562/A02 cells showed dose-effect dependence. The results demonstrated in **Figure 3B** indicated that with the absence of modulators, DOX accumulation in K562 cells was more than 4-fold ($p < 0.01$) than that in K562/A02 cells. In comparison, 0.1 μM compound **I-5** exhibited higher efficiency in enhancing accumulation of DOX in K562/A02 than VRP at 5 μM. Meanwhile, 5 μM **Tar** and **I-5** showed similar potency in increasing DOX accumulation in K562/A02, almost restored the DOX level to the parental K562's level. Results indicated that compound **I-5** was a potent P-gp inhibitor.

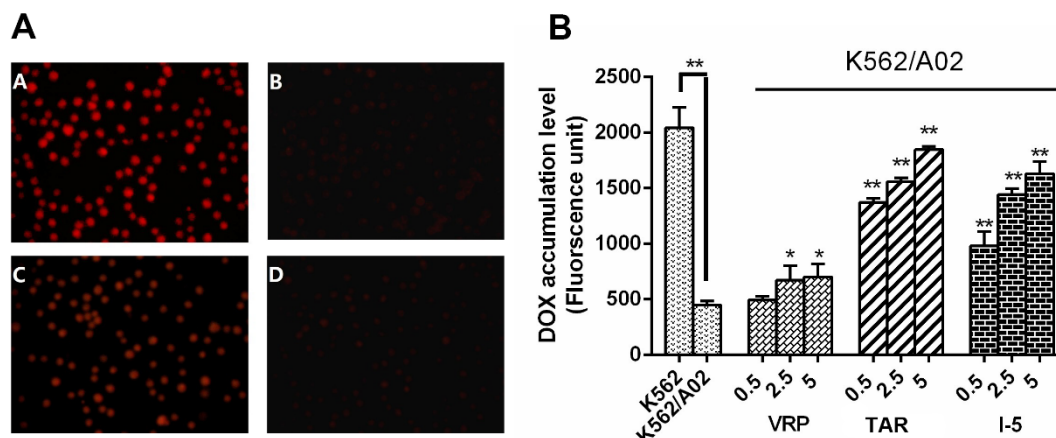


Figure 3. Effect of target compounds on intracellular DOX accumulation in K562 or K562/A02 cells. (A) with inverted fluorescence microscope: A) K562 cells + 20 μ M DOX; B) K562/A02 cells + 20 μ M DOX; C) K562/A02 cells + 5 μ M **I-5** + 20 μ M DOX; D) K562/A02 cells + 5 μ M VRP + 20 μ M DOX. (B) with fluorescence spectrophotometer. The results are presented as the mean \pm SD for three independent experiments; (**) $p < 0.01$, (*) $p < 0.05$ relative to the negative control (K562/A02).

2.6.2 Inhibitory effect on Rh123 efflux

Further exploration of the effect of **I-5** on P-gp efflux function was assayed by Rh123 efflux. As shown in Fig. 4, the efflux of Rh123 in the control group was increased during 90 min, while 2.0 μ M **I-5**-treated K562/A02 cells, the efflux of Rh123 was significantly inhibited, the remaining mean fluorescence intensity (MFI) at 90 min was over 50% compared with control and 5.0 μ M-treated VRP group, suggesting that **I-5** can reverse MDR by inhibiting P-gp-mediated drug efflux significantly..

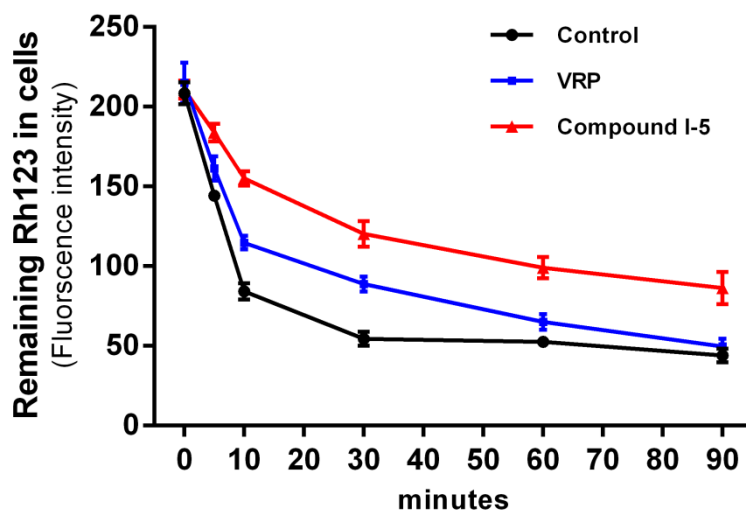


Figure 4. Effect of 2.0 μM I-5 and 5.0 μM VRP on efflux of Rh123 from K562/A02. Each data point is presented as mean \pm SD for three independent experiments.

2.7 Effect of I-5 on P-gp expression

The presence of P-gp protein was proved by a band with a molecular weight of ≈ 170 kDa in K562/A02 cell lysates by western blotting, while it was not present in parental K562 cells, suggesting the absence of P-gp protein (**Figure 5**). Inhibiting the function or lowering expression of P-gp will contribute to the reversal of P-gp-mediated MDR. Therefore, whether the reversal ability of I-5 was also due to a decrease in protein expression should be confirmed. As demonstrated in **Fig.5**, there was no significant alteration in P-gp expression in K562/A02 cells treated with different compounds or concentrations, indicating that MDR reversal by I-5 was not caused by a decreased P-gp expression but instead most likely due to direct inhibition of P-gp efflux.

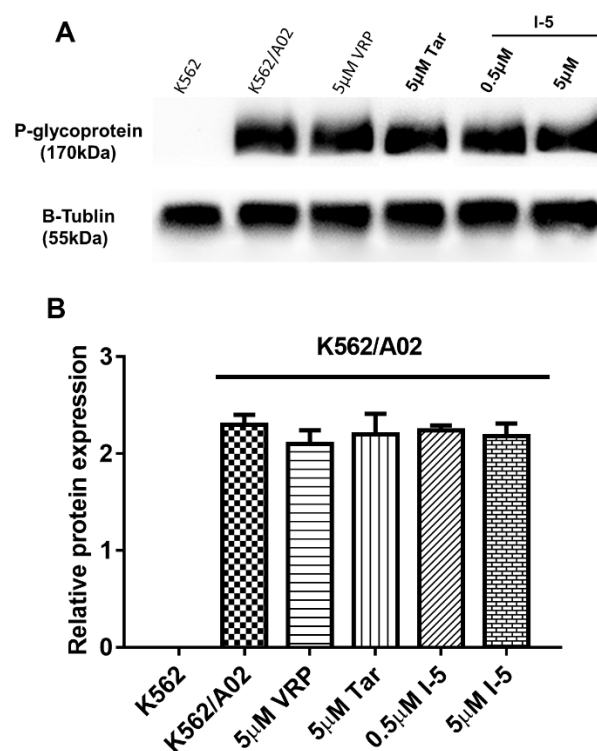


Figure 5. Western blot analysis showing the expression of ABCB1 after exposure to **I-5**. (A) Effect of **I-5** on expression level of ABCB1 in K562/A02 cells for 72 h. (B) Band intensity was analyzed by Quantity One software and protein expression was presented as the ratio of target protein's band intensity to that of β -Tubulin. Representative result is shown here, and similar results were obtained in two other independent trials.

3. Conclusion

In summary, in this paper, two series of triazole-tetrahydroisoquinoline-core P-gp inhibitors were designed and synthesized, series II was simplified based on series I. This investigation contributed to the identification of **I-5** as a potent P-gp inhibitor in reversing P-gp-mediated DOX-resistance in K562/A02 cells and possess outstanding reversal potency with EC_{50} in nanomolar range ($EC_{50} = 46.84 \pm 4.6$ nM). The longer duration of reversal activity was demonstrated in **I-5**, more than 24h.

Besides, **I-5** can significantly increase DOX accumulation in K562/A02 cells and suppress the efflux of Rh123 simultaneously. MDR reversal by **I-5** was not caused by a decreased P-gp expression but instead most likely due to direct inhibition of P-gp

efflux. As a result, **I-5** could be served as a promising candidate for the development of P-gp inhibitors in cancer chemotherapy.

4. Experimental Section

4.1 Reagents and apparatus

All starting materials, reagents and solvents were obtained from commercial sources and used without further purification unless otherwise indicated. Purifications by column chromatography were carried out over silica gel (200-300 mesh) and monitored by thin layer chromatography (TLC) performed on GF/UV 254 plates and were visualized using UV light at 254 and 365 nm. Melting points were taken on a RY-1 melting-point apparatus and were uncorrected. NMR spectra were recorded in DMSO-*d*₆ on a Bruker ACF-300Q instrument (300 MHz for ¹H, 75 MHz for ¹³C; Bruker Instruments, Inc., Billerica, MA, USA), chemical shifts are expressed as values (ppm) relative to tetramethylsilane as internal standard and coupling constants (*J* values) were given in hertz (Hz). Abbreviations are used as follows: s = singlet, d = doublet, t = triplet, q = quartet, m = multiplet, dd = doublets of doublet, br = broad. Infrared spectras were recorded on a Perkin-Elmer FTIR instrument. ESI-MS datas were recorded with Waters ACQUITY UPLC Systems with Mass (Waters, Milford, MA). The intermediates **a**, **b**, **c1-12**, **d**, **e**, **f**, **g**, **h**, **i**, and **j** were synthesized by previous reports[28,29].

4.2 General procedure for preparation of compounds **I-1-12** and **II-1-12**.

To the solution of **c1-12** (1mmol) and intermediates **g** or **i** (1mmol) in 75% methanol (40mL), ascorbate sodium (30mg) and CuSO₄ (10mg) were added. The crude product was purified by chromatography on silica gel utilized a mixture of chloroform and acetone (80:1, v/v) as eluent to furnish the desired target compounds **I-1-12** and **II-1-12**.

N-(2-(((1-(4-(2-(6,7-dimethoxy-3,4-dihydroisoquinolin-2(1*H*)-yl)ethyl)phenyl)-1*H*-1,2,3-triazol-4-yl)methyl)amino)phenyl)thiophene-2-carboxamide (**I-1**)

Yield: 39.6%; pale-yellow solid; m.p.107 - 109°C; ESI-MS *m/z*: 595.5 ([*M*+*H*]⁺); ¹H NMR (300 MHz, DMSO-*d*₆) δ ppm: 9.73 (s, 1H), 8.59 (s, 1H), 8.00 (s, 1H), 7.82 (s, 1H), 7.74 (d, *J* = 7.8 Hz, 2H), 7.47 (d, *J* = 7.4 Hz, 2H), 7.21 (s, 1H), 7.19 – 7.03 (m,

2H), 6.86 (d, $J = 7.8$ Hz, 1H), 6.64 (d, $J = 7.4$ Hz, 3H), 5.70 (t, $J = 4.4$ Hz, 1H), 4.46 (d, $J = 4.4$ Hz, 2H), 3.70 (s, 6H), 3.55 (s, 2H), 2.90 (s, 2H), 2.70 (s, 6H); ^{13}C NMR (75 MHz, DMSO- d_6) δ ppm: 160.53, 147.12, 146.82, 143.36, 141.22, 134.68, 131.29, 130.01, 129.19, 127.93, 127.57, 127.26, 120.99, 119.79, 116.23, 111.76, 111.49, 109.95, 58.99, 55.46, 55.00, 50.43, 38.94, 38.59, 32.26, 28.21; Anal. Calcd for $\text{C}_{33}\text{H}_{34}\text{N}_6\text{O}_3\text{S}$: C, 66.65; H, 5.76; N, 14.13. Found: C, 66.55; H, 5.64; N, 14.18.

***N*-(2-(((1-(4-(2-(6,7-dimethoxy-3,4-dihydroisoquinolin-2(1*H*)-yl)ethyl)phenyl)-1*H*-1,2,3-triazol-4-yl)methyl)amino)phenyl)thiophene-3-carboxamide (I-2)**

Yield: 45.3%; pale-yellow solid; m.p. 104 - 106 °C; ESI-MS m/z : 595.5 ($[\text{M}+\text{H}]^+$); ^1H NMR (300 MHz, DMSO- d_6) δ ppm: 9.55 (s, 1H), 8.58 (s, 1H), 8.32 (s, 1H), 7.80 - 7.68 (m, 2H), 7.63 (d, $J = 4.5$ Hz, 2H), 7.47 (d, $J = 6.3$ Hz, 2H), 7.13 (m, 2H), 6.86 (d, $J = 6.6$ Hz, 1H), 6.65 (d, $J = 6.0$ Hz, 3H), 5.58 (t, $J = 4.4$ Hz, 1H), 4.45 (d, $J = 4.4$ Hz, 2H), 3.70 (s, 6H), 3.55 (s, 2H), 2.90 (s, 2H), 2.70 (s, 6H); ^{13}C NMR (75 MHz, CDCl_3) δ ppm: 162.12, 147.51, 147.08, 142.14, 141.26, 135.13, 129.89, 129.41, 127.64, 126.44, 126.04, 124.38, 120.43, 120.10, 118.78, 113.85, 111.30, 109.40, 59.76, 56.18, 55.54, 51.04, 40.10, 33.50, 28.67; Anal. Calcd for $\text{C}_{33}\text{H}_{34}\text{N}_6\text{O}_3\text{S}$: C, 66.65; H, 5.76; N, 14.13. Found: C, 66.65; H, 5.64; N, 14.28.

***N*-(2-(((1-(4-(2-(6,7-dimethoxy-3,4-dihydroisoquinolin-2(1*H*)-yl)ethyl)phenyl)-1*H*-1,2,3-triazol-4-yl)methyl)amino)phenyl)-2-methylthiophene-3-carboxamide (I-3)**

Yield: 39.8%; pale-yellow solid; m.p. 89 - 91 °C; ESI-MS m/z : 609.3 ($[\text{M}+\text{H}]^+$); ^1H NMR (300 MHz, DMSO- d_6) δ ppm: 9.21 (s, 1H), 8.62 (s, 1H), 7.75 (d, $J = 8.0$ Hz, 2H), 7.65 (d, $J = 5.0$ Hz, 1H), 7.47 (d, $J = 8.0$ Hz, 2H), 7.21 (d, $J = 6.8$ Hz, 1H), 7.08 (d, $J = 7.4$ Hz, 1H), 7.02 (d, $J = 5.0$ Hz, 1H), 6.86 (d, $J = 7.4$ Hz, 1H), 6.65 (d, $J = 8.0$ Hz, 3H), 5.58 (t, $J = 5.4$ Hz, 1H), 4.45 (d, $J = 5.4$ Hz, 2H), 3.69 (s, 6H), 3.55 (s, 2H), 2.89 (d, $J = 6.8$ Hz, 2H), 2.70 (s, 6H), 2.48 (s, 3H); ^{13}C NMR (75 MHz, CDCl_3) δ ppm: 161.70, 147.12, 142.86, 142.60, 142.34, 141.86, 141.22, 135.25, 132.35, 129.92, 127.62, 127.34, 126.56, 125.70, 120.73, 120.53, 120.29, 119.05, 114.06, 111.32, 109.41, 76.89, 59.76, 55.81, 51.04, 40.26, 33.52, 28.65, 16.04; Anal. Calcd for $\text{C}_{34}\text{H}_{36}\text{N}_6\text{O}_3\text{S}$: C, 67.08; H, 5.96; N, 13.81. Found: C, 66.95; H, 5.94; N, 13.98.

***N*-2-(((1-(4-(2-(6,7-dimethoxy-3,4-dihydroisoquinolin-2(1*H*)-yl)ethyl)phenyl)-1*H*-1,2,3-triazol-4-yl)methyl)amino)phenyl)-5-methylthiophene-2-carboxamide (I-4)**

Yield: 45.3%; white solid; m.p.101 - 103°C; ESI-MS *m/z*: 609.3 ([*M*+*H*]⁺); ¹H NMR (300 MHz, DMSO-*d*6) δ ppm: 9.62 (s, 1H), 8.59 (s, 1H), 7.79 (s, 1H), 7.74 (d, *J* = 8.2 Hz, 2H), 7.46 (d, *J* = 8.1 Hz, 2H), 7.11 (m, 2H), 6.91 (s, 1H), 6.85 (d, *J* = 8.2 Hz, 1H), 6.64 (d, *J* = 7.8 Hz, 3H), 5.65 (t, *J* = 5.1 Hz, 1H), 4.45 (d, *J* = 5.1 Hz, 2H), 3.70 (s, 6H), 3.56 (s, 2H), 2.90 (s, 2H), 2.71 (s, 6H), 2.49 (s, 3H); ¹³C NMR (75 MHz, CDCl₃) δ ppm: 161.19, 147.14, 146.41, 141.20, 135.21, 129.90, 127.61, 126.90, 125.90, 120.46, 120.14, 118.88, 114.00, 111.32, 109.42, 59.75, 56.29, 55.54, 51.03, 40.21, 33.49, 28.64, 15.74; Anal. Calcd for C₃₄H₃₆N₆O₃S: C, 67.08; H, 5.96; N, 13.81. Found: C, 67.15; H, 6.04; N, 13.95.

***5*-chloro-*N*-2-(((1-(4-(2-(6,7-dimethoxy-3,4-dihydroisoquinolin-2(1*H*)-yl)ethyl)phenyl)-1*H*-1,2,3-triazol-4-yl)methyl)amino)phenyl)thiophene-2-carboxamide (I-5)**

Yield: 43.1%; pale-yellow solid; m.p.104 - 106°C; ESI-MS *m/z*: 629.3 ([*M*+*H*]⁺); ¹H NMR (300 MHz, DMSO-*d*6) δ ppm: 9.79 (s, 1H), 8.58 (s, 1H), 7.88 (s, 1H), 7.74 (d, *J* = 7.7 Hz, 2H), 7.46 (d, *J* = 7.0 Hz, 2H), 7.26 (s, 1H), 7.10 (t, *J* = 8.6 Hz, 2H), 6.85 (d, *J* = 8.0 Hz, 1H), 6.64 (d, *J* = 7.7 Hz, 3H), 5.76 (t, *J* = 5.0 Hz, 1H), 4.45 (d, *J* = 5.0 Hz, 2H), 3.69 (s, 6H), 3.54 (s, 2H), 2.90 (s, 2H), 2.70 (s, 6H); ¹³C NMR (75 MHz, DMSO-*d*6) δ ppm: 159.57, 146.77, 143.45, 141.24, 137.24, 134.90, 133.22, 130.01, 129.10, 128.75, 127.88, 126.55, 125.87, 122.58, 120.99, 119.78, 116.15, 111.76, 111.43, 109.94, 59.02, 55.45, 55.04, 50.46, 36.68, 32.27, 28.26; Anal. Calcd for C₃₃H₃₃ClN₆O₃S: C, 63.00; H, 5.29; N, 5.63. Found: C, 62.85; H, 5.34; N, 5.28.

***N*-2-(((1-(4-(2-(6,7-dimethoxy-3,4-dihydroisoquinolin-2(1*H*)-yl)ethyl)phenyl)-1*H*-1,2,3-triazol-4-yl)methyl)amino)phenyl)picolinamide (I-6)**

Yield: 33.6%; pale-yellow solid; m.p.144 - 146°C; ESI-MS *m/z*: 590.4 ([*M*+*H*]⁺); ¹H NMR (300 MHz, DMSO-*d*6) δ ppm: 10.09 (s, 1H), 8.73 (d, *J* = 4.1 Hz, 1H), 8.60 (s, 1H), 8.15 (d, *J* = 7.8 Hz, 1H), 8.05 (t, *J* = 7.3 Hz, 1H), 7.74 (d, *J* = 8.3 Hz, 2H), 7.70 - 7.61 (m, 1H), 7.46 (d, *J* = 8.3 Hz, 3H), 7.07 (t, *J* = 7.3 Hz, 1H), 6.87 (d, *J* = 8.3 Hz,

1H), 6.71 (t, $J = 7.3$ Hz, 1H), 6.64 (d, $J = 7.8$ Hz, 2H), 5.71 (t, $J = 5.4$ Hz, 1H), 4.44 (d, $J = 5.4$ Hz, 2H, -NHCH₂-), 3.70 (s, 6H, -OCH₃), 3.55 (s, 2H, -NCH₂Ar), 2.88 (d, $J = 7.1$ Hz, 2H), 2.70 (s, 6H); ¹³C NMR (75 MHz, DMSO-*d*₆) δ ppm: 162.78, 149.96, 148.36, 147.14, 146.83, 142.07, 141.20, 137.90, 134.72, 129.97, 126.70, 126.58, 126.47, 125.90, 125.45, 125.21, 124.29, 122.23, 121.01, 119.74, 117.00, 112.32, 111.78, 109.99, 58.98, 55.46, 55.01, 50.43, 32.27, 28.23; Anal. Calcd for C₃₄H₃₅N₇O₃: C, 69.25; H, 5.98; N, 16.63. Found: C, 69.35; H, 5.90; N, 16.78.

***N*-(2-(((1-(4-(2-(6,7-dimethoxy-3,4-dihydroisoquinolin-2(1*H*)-yl)ethyl)phenyl)-1*H*-1,2,3-triazol-4-yl)methyl)amino)phenyl)isonicotinamide (I-7)**

Yield: 29.8%; brown solid; m.p.178 - 180 °C; ESI-MS m/z : 590.3 ([M+H]⁺); ¹H NMR (300 MHz, , DMSO-*d*₆) δ ppm: 9.92 (s, 1H), 8.58 (s, 1H), 7.74 (s, 3H), 7.46 (s, 3H), 7.30 (s, 1H), 7.16 (s, 2H), 7.11 (s, 2H), 6.84 (s, 1H), 6.65 (s, 4H), 5.79 (t, $J = 5.4$ Hz, 1H), 4.45(d, $J = 5.4$ Hz, 2H), 3.70 (s, 6H), 2.90 (d, $J = 7.1$ Hz, 2H), 2.73 (s, 6H); ¹³C NMR (75 MHz, DMSO-*d*₆) δ ppm: 164.19, 150.07, 147.14, 146.85, 145.49, 143.28, 141.59, 127.38, 126.23, 125.78, 122.90, 121.78, 115.86, 111.74, 111.27, 109.84, 56.76, 55.43, 54.87, 50.04, 46.97, 40.82 – 40.53, 40.14, 39.59, 39.18, 39.18, 28.02; Anal. Calcd for C₃₄H₃₅N₇O₃: C, 69.25; H, 5.98; N, 16.63. Found: C, 69.45; H, 5.86; N, 16.68.

***2*-chloro-*N*-(2-(((1-(4-(2-(6,7-dimethoxy-3,4-dihydroisoquinolin-2(1*H*)-yl)ethyl)phenyl)-1*H*-1,2,3-triazol-4-yl)methyl)amino)phenyl)nicotinamide (I-8)**

Yield: 34.5%; white solid; m.p.129 - 131 °C; ESI-MS m/z : 624.3 ([M+H]⁺); ¹H NMR (300 MHz, DMSO-*d*₆) δ ppm: 9.88 (s, 1H), 8.63 (s, 1H), 8.52 (s, 1H), 8.17 (d, $J = 7.5$ Hz, 1H), 7.75 (d, $J = 6.3$ Hz, 2H), 7.57 (s, 1H), 7.47 (d, $J = 6.4$ Hz, 2H), 7.34 (d, $J = 7.5$ Hz, 1H), 7.12 (s, 1H), 6.88 (d, $J = 6.4$ Hz, 1H), 6.69 (s, 1H), 6.65 (m, 2H), 5.47 (t, $J = 5.4$ Hz, 1H), 4.47 (d, $J = 5.4$ Hz, 2H), 3.70 (s, 6H), 3.55 (s, 2H), 2.90 (s, 2H), 2.71 (s, 6H); ¹³C NMR (75 MHz, CDCl₃) δ ppm: 159.23, 146.32, 143.37, 142.81, 142.62, 141.83, 137.19, 136.62, 134.83, 130.37, 126.77, 125.20, 123.41, 121.91, 121.69, 121.43, 118.70, 118.06, 115.72, 115.26, 114.07, 108.80, 106.59, 104.69, 54.97, 51.49, 50.77, 46.28, 35.32, 28.73, 23.89; Anal. Calcd for C₃₄H₃₄ClN₇O₃: C, 65.43; H, 5.49; N, 15.71. Found: C, 65.35; H, 5.64; N, 15.88.

***N*-(2-(((1-(4-(2-(6,7-dimethoxy-3,4-dihydroisoquinolin-2(1*H*)-yl)ethyl)phenyl)-1*H*-1,2,3-triazol-4-yl)methyl)amino)phenyl)-1*H*-indole-2-carboxamide (I-9)**

Yield: 38.1%; orange solid; m.p.126 - 128°C ; ESI-MS *m/z*: 626.9 ([*M*-1]⁺); ¹H NMR (300 MHz, DMSO-*d*6) δ ppm: 11.70 (s, 1H), 9.74 (s, 1H), 8.61 (s, 1H), 7.74 (s, 2H), 7.68 (s, 1H), 7.47 (d, *J* = 7.4 Hz, 3H), 7.37 (s, 1H), 7.28 – 7.16 (m, 2H), 7.16 – 6.99 (m, 2H), 6.90 (s, 1H), 6.65 (d, *J* = 7.4 Hz, 3H), 5.80 – 5.58 (t, *J* = 5.4 Hz, 1H), 4.47 (d, *J* = 5.4 Hz, 2H), 3.70 (s, 6H), 3.57 (s, 2H), 2.90 (s, 2H), 2.72 (s, 6H); ¹³C NMR (75 MHz, CDCl₃) δ ppm: 153.14, 142.15, 141.32, 139.05, 137.45, 136.60, 131.72, 130.59, 129.60, 124.76, 123.26, 121.09, 120.81, 118.83, 118.18, 116.29, 115.31, 114.91, 106.49, 106.10, 104.48, 98.73, 54.41, 51.04, 50.29, 45.76, 35.69, 28.25, 23.40; Anal. Calcd for C₃₇H₃₇N₇O₃: C, 70.79; H, 5.94; N, 15.62. Found: C, 70.75; H, 5.84; N, 15.48.

***N*-(2-(((1-(4-(2-(6,7-dimethoxy-3,4-dihydroisoquinolin-2(1*H*)-yl)ethyl)phenyl)-1*H*-1,2,3-triazol-4-yl)methyl)amino)phenyl)quinoline-3-carboxamide (I-10)**

Yield: 37.2%; pale-yellow solid; m.p.109 - 111°C ; ESI-MS *m/z*: 640.4([*M*+H]⁺); ¹H NMR (300 MHz, DMSO-*d*6) δ ppm: 10.02 (s, 1H), 9.43 (s, 1H), 9.01 (s, 1H), 8.61 (s, 1H), 8.18 – 8.09 (m, 2H), 7.93 – 7.85 (m, 1H), 7.74 (d, *J* = 8.2 Hz, 3H), 7.46 (d, *J* = 8.2 Hz, 2H), 7.25 (d, *J* = 7.4 Hz, 1H), 7.12 (t, *J* = 7.4 Hz, 1H), 6.88 (d, *J* = 7.9 Hz, 1H), 6.69 (d, *J* = 7.0 Hz, 1H), 6.64 (d, *J* = 7.9 Hz, 2H), 5.91 (t, *J* = 5.2 Hz, 1H), 4.49 (d, *J* = 5.2 Hz, 2H), 3.69 (s, 6H), 3.54 (s, 2H), 2.94 – 2.84 (m, 2H), 2.70 (s, 6H); ¹³C NMR (75 MHz, DMSO-*d*6) δ ppm: 164.52, 153.30, 149.38, 148.40, 147.01, 143.30, 141.24, 138.59, 136.16, 134.71, 131.21, 130.00, 129.10, 128.93, 127.50, 127.37, 126.57, 125.88, 123.24, 121.00, 119.77, 116.14, 111.75, 111.42, 109.95, 59.02, 55.50, 55.26, 50.44, 38.52, 32.28, 28.26; Anal. Calcd for C₃₈H₃₇N₇O₃: C, 71.34; H, 5.83; N, 15.33. Found: C, 71.25; H, 5.66; N, 15.25.

***N*-(2-(((1-(4-(2-(6,7-dimethoxy-3,4-dihydroisoquinolin-2(1*H*)-yl)ethyl)phenyl)-1*H*-1,2,3-triazol-4-yl)methyl)amino)phenyl)quinoline-2-carboxamide (I-11)**

Yield 39.5%; yellow solid; m.p.136 - 138°C ; ESI-MS *m/z*: 640.4 ([*M*+H]⁺); ¹H NMR (300 MHz, DMSO-*d*6) δ ppm: 10.28 (s, 1H), 8.63 (m, 2H), 8.25 (d, *J* = 8.4 Hz, 1H), 8.15 (d, *J* = 8.4 Hz, 2H), 7.83 (d, *J* = 7.2 Hz, 1H), 7.75 (s, 3H), 7.55 (d, *J* = 7.2 Hz,

1H), 7.47 (d, $J = 7.6$ Hz, 2H), 7.11 (s, 1H), 6.92 (d, $J = 7.6$ Hz, 1H), 6.76 (s, 1H), 6.65 (d, $J = 7.2$ Hz, 2H), 5.79 (t, $J = 5.2$ Hz, 1H), 4.46 (d, $J = 5.2$ Hz), 3.70 (s, 6H), 3.56 (s, 2H), 2.91 (s, 2H), 2.71 (s, 6H); ^{13}C NMR (75 MHz, DMSO- d_6) δ ppm: 162.90, 150.14, 147.05, 145.85, 142.07, 141.21, 137.96, 134.75, 130.47, 129.99, 129.27, 128.87, 128.11, 126.58, 126.50, 125.90, 125.22, 124.55, 121.04, 119.78, 118.73, 117.23, 112.64, 111.83, 110.02, 58.99, 55.49, 55.03, 50.44, 38.98, 32.27, 28.25; Anal. Calcd for $\text{C}_{38}\text{H}_{37}\text{N}_7\text{O}_3$: C, 71.34; H, 5.83; N, 15.33. Found: C, 71.40; H, 5.96; N, 15.35.

***N*-(2-(((1-(4-(2-(6,7-dimethoxy-3,4-dihydroisoquinolin-2(1*H*)-yl)ethyl)phenyl)-1*H*-1,2,3-triazol-4-yl)methyl)amino)phenyl)furan-2-carboxamide (I-12)**

Yield: 29.6%; pale-yellow solid; m.p. 94 - 96°C; ESI-MS m/z : 579.3 ($[\text{M}+\text{H}]^+$); ^1H NMR (300 MHz, DMSO- d_6) δ ppm: 9.57 (s, 1H), 8.57 (s, 1H), 7.90 (s, 1H), 7.74 (d, $J = 8.3$ Hz, 2H), 7.46 (d, $J = 8.3$ Hz, 2H), 7.29 (s, 1H), 7.17 (d, $J = 7.4$ Hz, 1H), 7.09 (t, $J = 7.4$ Hz, 1H), 6.84 (d, $J = 8.0$ Hz, 1H), 6.73 – 6.59 (m, 4H), 5.66 (t, $J = 5.4$ Hz, 1H), 4.45 (d, $J = 5.4$ Hz, 2H), 3.70 (s, 6H), 3.55 (s, 2H), 2.89 (d, $J = 7.4$ Hz, 2H), 2.70 (s, 6H); ^{13}C NMR (75 MHz, DMSO- d_6) δ ppm: 162.44, 147.77, 146.88, 145.28, 143.16, 138.59, 136.82, 130.00, 127.19, 126.50, 125.98, 125.71, 122.96, 121.00, 119.78, 116.86, 116.30, 114.34, 111.89, 110.02, 59.00, 55.47, 55.03, 50.45, 37.04, 32.29, 28.24; Anal. Calcd for $\text{C}_{33}\text{H}_{39}\text{N}_6\text{O}_4$: C, 68.50; H, 5.92; N, 14.52. Found: C, 68.55; H, 5.84; N, 14.48.

***N*-(2-(((1-(2-(6,7-dimethoxy-3,4-dihydroisoquinolin-2(1*H*)-yl)ethyl)-1*H*-1,2,3-triazol-4-yl)methyl)amino)phenyl)thiophene-2-carboxamide (II-1)**

Yield: 35.4%; pale-yellow solid; m.p. 94 - 96°C; ESI-MS m/z : 519.4 ($[\text{M}+\text{H}]^+$); ^1H NMR (300 MHz, DMSO- d_6) δ ppm: 9.68 (s, 1H), 7.94 (d, $J = 7.5$ Hz, 2H), 7.82 (s, 1H), 7.17 (m, 2H, ArH), 7.04 (d, $J = 7.5$ Hz, 1H), 6.78 (s, 1H), 6.63 (s, 3H), 5.55 (t, $J = 5.7$ Hz, 1H), 4.52 (t, $J = 6.0$ Hz, 2H), 4.36 (d, $J = 5.7$ Hz, 2H), 3.69 (s, 6H), 3.52 (s, 2H), 2.87 (t, $J = 6.0$ Hz, 2H), 2.64 (s, 4H); ^{13}C NMR (75 MHz, DMSO- d_6) δ ppm: 160.38, 147.22, 147.06, 145.38, 143.33, 139.72, 131.23, 129.13, 127.92, 127.64, 127.10, 126.29, 125.83, 122.99, 116.05, 111.88, 111.42, 109.97, 56.72, 55.50, 54.85, 50.07, 47.02, 40.10, 38.98, 38.67, 28.01; Anal. Calcd for $\text{C}_{27}\text{H}_{30}\text{N}_6\text{O}_3\text{S}$: C, 62.53; H,

5.83; N, 16.20. Found: C, 62.58; H, 5.80; N, 16.13.

***N*-(2-(((1-(2-(6,7-dimethoxy-3,4-dihydroisoquinolin-2(1*H*)-yl)ethyl)-1*H*-1,2,3-triazol-4-yl)methyl)amino)phenyl)thiophene-3-carboxamide (II-2)**

Yield: 33.5%; pale-yellow solid; m.p. 95 - 97°C; ESI-MS *m/z*: 519.4 ([M+H]⁺); ¹H NMR (300 MHz, DMSO-*d*₆) δ ppm: 9.52 (s, 1H), 8.29 (s, 1H), 7.93 (s, 1H), 7.62 (s, 2H), 7.13 (d, *J* = 6.4 Hz, 1H), 7.03 (t, *J* = 7.5 Hz, 1H), 6.76 (d, *J* = 7.5 Hz, 1H), 6.63 (s, 2H), 6.57 (s, 1H), 5.52 (t, *J* = 5.7 Hz, 1H), 4.51 (t, *J* = 6.0 Hz, 2H), 4.35 (d, *J* = 5.7 Hz, 2H), 3.75 – 3.62 (s, 6H), 3.51 (s, 2H), 2.86 (t, *J* = 6.0 Hz, 2H), 2.64 (s, 4H); ¹³C NMR (75 MHz, DMSO-*d*₆) δ ppm: 161.51, 147.42, 146.90, 145.41, 143.22, 139.23, 129.52, 127.28, 126.94, 126.55, 125.82, 123.41, 123.00, 116.07, 111.85, 111.40, 109.97, 56.72, 55.50, 54.85, 50.06, 47.01, 42.50, 40.33, 38.96, 38.67, 28.00; Anal. Calcd for C₂₇H₃₀N₆O₃S: C, 62.53; H, 5.83; N, 16.20. Found: C, 62.48; H, 5.85; N, 16.25.

***N*-(2-(((1-(2-(6,7-dimethoxy-3,4-dihydroisoquinolin-2(1*H*)-yl)ethyl)-1*H*-1,2,3-triazol-4-yl)methyl)amino)phenyl)-3-methylthiophene-2-carboxamide (II-3)**

Yield: 47.5%; pale-yellow solid; m.p. 84 - 86°C; ESI-MS *m/z*: 555.6 ([M+ Na]⁺); ¹H NMR (300 MHz, DMSO-*d*₆) δ ppm: 9.18 (s, 1H), 7.95 (s, 1H), 7.64 (d, *J* = 4.5 Hz, 1H), 7.20 (d, *J* = 6.8 Hz, 1H), 7.00 (d, *J* = 4.5 Hz, 2H), 6.77 (d, *J* = 6.8 Hz, 1H), 6.63 (s, 2H), 6.58 (s, 1H), 5.43 (t, *J* = 4.5 Hz, 1H), 4.53 (t, *J* = 4.8 Hz, 2H), 4.34 (d, *J* = 4.5 Hz, 2H), 3.69 (s, 6H), 3.52 (s, 2H), 2.87 (t, *J* = 4.8 Hz, 2H), 2.64 (s, 4H), 2.45 (s, 3H); ¹³C NMR (75 MHz, CDCl₃) δ ppm: 161.61, 145.98, 132.29, 127.26, 125.90, 125.58, 122.53, 119.06, 114.32, 111.33, 109.33, 57.11, 55.91, 55.48, 50.82, 47.99, 40.38, 28.47, 15.99; Anal. Calcd for C₂₈H₃₂N₆O₃S: C, 63.14; H, 6.06; N, 15.78. Found: C, 63.05; H, 6.09; N, 15.83.

***N*-(2-(((1-(2-(6,7-dimethoxy-3,4-dihydroisoquinolin-2(1*H*)-yl)ethyl)-1*H*-1,2,3-triazol-4-yl)methyl)amino)phenyl)-5-methylthiophene-2-carboxamide (II-4)**

Yield: 35.9%; brown solid; m.p. 92 - 94°C; ESI-MS *m/z*: 555.6 ([M+ Na]⁺); ¹H NMR (300 MHz, DMSO-*d*₆) δ ppm: 9.57 (s, 1H), 7.93 (s, 1H), 7.77 (s, 1H), 7.12 (d, *J* = 6.3 Hz, 1H), 7.07 – 6.98 (m, 1H), 6.90 (s, 1H), 6.75 (d, *J* = 6.3 Hz, 1H), 6.63 (s, 2H), 6.58 (s, 1H), 5.51 (t, *J* = 4.5 Hz, 1H), 4.52 (t, *J* = 4.8 Hz, 2H), 4.35 (d, *J* = 4.5 Hz, 2H),

3.69 (s, 6H), 3.52 (s, 2H), 2.87 (t, $J = 4.8$ Hz, 2H), 2.64 (s, 4H), 2.46 (s, 3H); ^{13}C NMR (75 MHz, DMSO-*d*6) δ ppm: 160.32, 147.15, 146.86, 145.35, 143.24, 129.40, 127.30, 126.98, 126.41, 126.23, 126.55, 125.72, 125.43, 123.17, 123.09, 123.01, 116.07, 111.78, 111.40, 109.88, 56.72, 55.45, 54.83, 50.05, 46.97, 38.64, 27.99, 15.23; Anal. Calcd for $\text{C}_{28}\text{H}_{32}\text{N}_6\text{O}_3\text{S}$: C, 63.14; H, 6.06; N, 15.78. Found: C, 63.22; H, 6.01; N, 15.76.

5-chloro-*N*-(2-(((1-(2-(6,7-dimethoxy-3,4-dihydroisoquinolin-2(1*H*)-yl)ethyl)-1*H*-1,2,3-triazol-4-yl)methyl)amino)phenyl)thiophene-2-carboxamide (II-5)

Yield: 32.3%; pale-yellow solid; m.p. 93 - 95°C ; ESI-MS m/z : 553.4([M+H]⁺); ^1H NMR (300 MHz, DMSO-*d*6) δ ppm: 9.74 (s, 1H), 7.90 (s, 1H), 7.83 (s, 1H), 7.23 (d, $J = 7.8$ Hz, 1H), 7.05 (d, $J = 6.6$ Hz, 2H), 6.74 (d, $J = 7.8$ Hz, 1H), 6.62 (s, 2H), 6.56 (s, 1H), 5.52 (t, $J = 4.5$ Hz, 1H), 4.49 (t, $J = 4.8$ Hz, 2H), 4.34 (d, $J = 4.5$ Hz, 2H), 3.67 (s, 6H), 3.50 (s, 2H), 2.84 (t, $J = 4.8$ Hz, 2H), 2.63 (s, 4H); ^{13}C NMR (75 MHz, DMSO-*d*6) δ ppm: 159.28, 147.18, 146.88, 145.38, 143.40, 138.24, 136.82, 133.16, 129.03, 128.02, 127.38, 126.03, 125.43, 122.72, 122.14, 119.78, 115.94, 111.57, 109.91, 56.72, 55.47, 54.85, 50.03, 46.98, 38.57, 28.00; Anal. Calcd for $\text{C}_{27}\text{H}_{29}\text{ClN}_6\text{O}_3\text{S}$: C, 58.63; H, 5.29; N, 15.20. Found: C, 58.76; H, 5.21; N, 15.16.

***N*-(2-(((1-(2-(6,7-dimethoxy-3,4-dihydroisoquinolin-2(1*H*)-yl)ethyl)-1*H*-1,2,3-triazol-4-yl)methyl)amino)phenyl)picolinamide (II-6)**

Yield: 23.5%; brown solid; m.p. 133 - 135°C ; ESI-MS m/z : 536.5 ([M+Na]⁺); ^1H NMR (300 MHz, DMSO-*d*6) δ ppm: 10.09 (s, 1H), 8.72 (d, $J = 4.5$ Hz, 1H), 8.13 (d, $J = 7.7$ Hz, 1H), 8.05 (t, $J = 7.6$ Hz, 1H), 7.96 (s, 1H), 7.69 - 7.63 (m, 1H), 7.45 (d, $J = 7.7$ Hz, 1H), 7.01 (t, $J = 7.6$ Hz, 1H), 6.78 (d, $J = 8.1$ Hz, 1H), 6.69 (t, $J = 7.6$ Hz, 1H), 6.62 (s, 1H), 6.57 (s, 1H), 5.65 (t, $J = 5.5$ Hz, 1H), 4.52 (t, $J = 5.8$ Hz, 2H), 4.34 (d, $J = 5.5$ Hz, 2H), 3.68 (s, 6H), 3.51 (s, 2H), 2.86 (t, $J = 5.8$ Hz, 2H), 2.62 (s, 4H); ^{13}C NMR (75 MHz, DMSO-*d*6) δ ppm: 162.59, 149.91, 149.11, 148.37, 146.84, 145.44, 141.97, 137.92, 126.70, 126.23, 125.75, 125.21, 124.26, 123.10, 122.19, 116.84, 112.31, 111.74, 109.85, 56.76, 55.43, 54.84, 50.08, 46.99, 36.68, 28.00; Anal. Calcd for $\text{C}_{28}\text{H}_{31}\text{N}_7\text{O}_3$: C, 65.48; H, 6.08; N, 19.09. Found: C, 65.41; H, 6.11; N, 19.06.

***N*-(2-(((1-(2-(6,7-dimethoxy-3,4-dihydroisoquinolin-2(1*H*)-yl)ethyl)-1*H*-1,2,3-triazol-4-yl)methyl)amino)phenyl)isonicotinamide (II-7)**

Yield: 28.9%; pale-yellow solid; m.p. 98 - 100 °C; ESI-MS *m/z*: 536.5 ([*M*+*Na*]⁺); ¹H NMR (300 MHz, DMSO-*d*₆) δ ppm: 9.90 (s, 1H), 8.77 (d, *J* = 3.6 Hz, 2H), 7.93 (s, 1H), 7.91 (s, 1H), 7.89 (s, 1H), 7.17 (d, *J* = 7.5 Hz, 1H), 7.05 (t, *J* = 7.2 Hz, 1H), 6.77 (d, *J* = 8.0 Hz, 1H), 6.66 – 6.60 (m, 2H), 6.57 (s, 1H), 5.69 (t, *J* = 5.7 Hz, 1H), 4.52 (t, *J* = 6.0 Hz, 2H), 4.36 (d, *J* = 5.7 Hz, 2H), 3.69 (s, 6H), 3.51 (s, 2H), 2.86 (t, *J* = 6.0 Hz, 2H), 2.64 (s, 4H); ¹³C NMR (75 MHz, DMSO-*d*₆) δ ppm: 164.19, 150.06, 147.16, 146.86, 145.49, 143.27, 141.59, 127.35, 126.24, 125.79, 123.02, 122.77, 121.79, 115.87, 111.76, 111.28, 109.86, 56.76, 55.44, 54.87, 50.04, 46.98, 28.03; Anal. Calcd for C₂₈H₃₁N₇O₃: C, 65.48; H, 6.08; N, 19.09. Found: C, 65.51; H, 6.13; N, 19.01.

***2*-chloro-*N*-(2-(((1-(2-(6,7-dimethoxy-3,4-dihydroisoquinolin-2(1*H*)-yl)ethyl)-1*H*-1,2,3-triazol-4-yl)methyl)amino)phenyl)nicotinamide (II-8)**

Yield: 33.5%; pale-yellow solid; m.p. 99 - 101 °C; ESI-MS *m/z*: 570.5 ([*M*+*Na*]⁺); ¹H NMR (300 MHz, DMSO-*d*₆) δ ppm: 9.88 (s, 1H), 8.53 (s, 1H), 8.15 (s, 1H), 7.98 (d, *J* = 6.0 Hz, 1H), 7.56 (d, *J* = 7.2 Hz, 1H), 7.33 (d, *J* = 6.0 Hz, 1H), 7.06 (s, 1H), 6.79 (d, *J* = 7.2 Hz, 1H), 6.73 – 6.61 (m, 2H), 6.58 (s, 1H), 5.42 (t, *J* = 4.5 Hz, 2H, 1H), 4.54 (t, *J* = 6.0 Hz, 2H), 4.38 (d, *J* = 4.5 Hz, 2H), 3.69 (s, 6H), 3.53 (s, 2H), 2.88 (t, *J* = 6.0 Hz, 2H), 2.65 (s, 4H); ¹³C NMR (75 MHz, CDCl₃) δ ppm: 150.99, 147.23, 145.60, 141.86, 139.57, 131.60, 127.93, 125.86, 123.58, 122.80, 122.52, 118.70, 113.63, 111.32, 109.34, 57.10, 55.91, 55.47, 50.81, 47.96, 40.09, 28.48; Anal. Calcd for C₂₈H₃₀ClN₇O₃: C, 61.37; H, 5.52; N, 17.89. Found: C, 61.32; H, 5.50; N, 17.95.

***N*-(2-(((1-(2-(6,7-dimethoxy-3,4-dihydroisoquinolin-2(1*H*)-yl)ethyl)-1*H*-1,2,3-triazol-4-yl)methyl)amino)phenyl)-1*H*-indole-2-carboxamide (II-9)**

Yield: 38.9%; pale-green solid; m.p. 115 - 117 °C; ESI-MS *m/z*: 552.5 ([*M*+*H*]⁺); ¹H NMR (300 MHz, DMSO-*d*₆) δ ppm: 11.69 (s, 1H), 9.70 (s, 1H), 7.96 (s, 1H), 7.66 (d, *J* = 8.0 Hz, 1H), 7.48 (d, *J* = 8.0 Hz, 1H), 7.36 (s, 1H), 7.22 (t, *J* = 7.3 Hz, 2H), 7.07 (t, *J* = 7.5 Hz, 2H), 6.82 (d, *J* = 8.0 Hz, 1H), 6.68 (t, *J* = 7.5 Hz, 1H), 6.59 (s, 1H), 6.56 (s, 1H), 5.57 (t, *J* = 5.2 Hz, 1H), 4.52 (t, *J* = 5.4 Hz, 2H), 4.37 (d, *J* = 5.2 Hz, 2H),

3.68 (s, 6H), 3.51 (s, 2H), 2.87 (t, $J = 5.4$ Hz, 2H), 2.62 (s, 4H); ^{13}C NMR (75 MHz, DMSO-*d*₆) δ ppm: 160.27, 147.16, 146.87, 145.29, 143.16, 136.62, 131.47, 127.05, 126.23, 125.77, 123.55, 123.15, 121.57, 119.83, 116.24, 112.34, 111.66, 109.86, 103.81, 56.74, 55.44, 54.82, 50.08, 47.01, 38.83, 28.24, 27.99; Anal. Calcd for $\text{C}_{31}\text{H}_{33}\text{N}_7\text{O}_3$: C, 67.50; H, 6.03; N, 17.77. Found: C, 67.59; H, 6.01; N, 17.72.

***N*-(2-(((1-(2-(6,7-dimethoxy-3,4-dihydroisoquinolin-2(1*H*)-yl)ethyl)-1*H*-1,2,3-triazol-4-yl)methyl)amino)phenyl)quinoline-3-carboxamide (II-10)**

Yield: 37.5%; pale-yellow solid; m.p. 105 - 107 °C; ESI-MS m/z : 564.5 ($[\text{M}+\text{H}]^+$); ^1H NMR (300 MHz, DMSO-*d*₆) δ ppm: 9.99 (s, 1H), 9.41 (s, 1H), 8.99 (s, 1H), 8.13 (s, 2H), 7.94 (s, 2H), 7.73 (s, 1H), 7.23 (s, 1H), 7.06 (s, 1H), 6.78 (s, 1H), 6.75 – 6.48 (m, 3H), 5.76 (t, $J = 5.4$ Hz, 1H), 4.51 (t, $J = 5.4$ Hz, 2H), 4.38 (d, $J = 5.2$ Hz, 2H), 3.67 (s, 6H), 3.50 (s, 2H), 2.86 (t, $J = 5.4$ Hz, 2H), 2.62 (s, 4H); ^{13}C NMR (75 MHz, DMSO-*d*₆) δ ppm: 165.45, 149.36, 148.55, 147.03, 145.53, 143.30, 136.10, 131.18, 130.67, 130.46, 129.09, 128.76, 127.29, 126.82, 126.48, 126.03, 123.08, 115.93, 111.80, 111.31, 109.91, 56.73, 55.46, 54.88, 50.01, 46.99, 38.77, 38.65, 28.00; Anal. Calcd for $\text{C}_{32}\text{H}_{33}\text{N}_7\text{O}_3$: C, 68.19; H, 5.90; N, 17.39. Found: C, 68.26; H, 5.93; N, 17.31.

***N*-(2-(((1-(2-(6,7-dimethoxy-3,4-dihydroisoquinolin-2(1*H*)-yl)ethyl)-1*H*-1,2,3-triazol-4-yl)methyl)amino)phenyl)quinoline-3-carboxamide (II-11)**

Yield: 45.3%; yellow solid; m.p. 94 - 95 °C; ESI-MS m/z : 586.7 ($[\text{M}+\text{Na}]^+$); ^1H NMR (300 MHz, DMSO-*d*₆) δ ppm: 10.22 (s, 1H), 8.61 (d, $J = 7.8$ Hz, 1H), 8.28 – 8.16 (m, 2H), 8.11 (d, $J = 7.3$ Hz, 1H), 7.98 (s, 1H), 7.91 (d, $J = 6.4$ Hz, 1H), 7.76 (d, $J = 6.4$ Hz, 1H), 7.50 (d, $J = 6.7$ Hz, 1H), 7.06 (d, $J = 5.7$ Hz, 1H), 6.83 (d, $J = 7.3$ Hz, 1H), 6.73 (d, $J = 6.4$ Hz, 1H), 6.59 (s, 1H), 6.54 (s, 1H), 5.71 (t, $J = 5.4$ Hz, 1H), 4.52 (t, $J = 5.4$ Hz, 2H), 4.38 (d, $J = 5.2$ Hz, 2H), 3.67 (s, 6H), 3.50 (s, 2H), 2.86 (t, $J = 5.4$ Hz, 2H), 2.61 (s, 4H); ^{13}C NMR (75 MHz, DMSO-*d*₆) δ ppm: 162.87, 150.13, 147.18, 146.89, 145.87, 145.52, 142.18, 137.93, 130.54, 129.30, 128.87, 128.13, 126.37, 125.78, 125.35, 124.22, 123.05, 120.39, 118.73, 116.90, 112.42, 111.81, 109.92, 56.74, 55.47, 54.83, 50.07, 47.05, 36.68, 27.99; Anal. Calcd for $\text{C}_{32}\text{H}_{33}\text{N}_7\text{O}_3$: C, 68.19; H, 5.90; N, 17.39. Found: C, 68.10; H, 5.88; N, 17.44.

***N*-(2-(((1-(2-(6,7-dimethoxy-3,4-dihydroisoquinolin-2(1*H*)-yl)ethyl)-1*H*-1,2,3-**

triazol-4-yl)methyl)amino)phenyl)furan-2-carboxamide (II-12)

Yield: 39.6%; pale-yellow solid; m.p. 96 - 98°C; ESI-MS m/z : 503.3 ($[M+H]^+$); 1H NMR (300 MHz, DMSO- d_6) δ ppm: 9.55 (s, 1H), 7.92 (d, $J = 11.1$ Hz, 2H), 7.26 (s, 1H), 7.15 (d, $J = 7.3$ Hz, 1H), 7.03 (t, $J = 7.5$ Hz, 1H), 6.75 (d, $J = 8.1$ Hz, 1H), 6.63 (m, 4H), 5.55 (t, $J = 5.4$ Hz, 1H), 4.52 (t, $J = 5.4$ Hz, 2H), 4.34 (d, $J = 4.8$ Hz, 2H), 3.69 (s, 6H), 3.52 (s, 2H), 2.87 (t, $J = 5.4$ Hz, 2H), 2.64 (s, 4H); ^{13}C NMR (75 MHz, DMSO- d_6) δ ppm: 156.80, 147.74, 147.16, 146.86, 145.32, 143.14, 127.06, 126.25, 125.78, 122.94, 118.99, 116.11, 114.31, 111.86, 111.48, 109.88, 56.74, 55.45, 54.84, 50.08, 46.99, 38.65, 27.99; Anal. Calcd for $C_{27}H_{30}N_6O_4$: C, 64.53; H, 6.02; N, 16.72. Found: C, 64.46; H, 5.98; N, 16.80.

4.2 Molecular docking studies

P-gp protein (PDB ID: 6FN1) was set out and optimized with relevant module by Schrodinger software. Receptor Grid Generation Module was utilized to produce docking area. Structure of ligands were drawn by ChemOffice2017 software and prepared using LigPrep module. Ultimately, molecular docking between ligands and receptor was conducted with extra precision.

4.3 Cytotoxicity and MDR reversal assay

The cell viability was tested by MTT assay with a minor modification.[30-32] K562 and K562/A02 cells were harvested during logarithmic growth phase, and were seeded in 96-well micro-titer plates at 1×10^4 cells per well. In the MTT assay for anticancer MDR reversal experiments, cells were exposed to the presence of DOX with or without P-gp inhibitors for 48 h. MTT dye (10 μ l of 2.5 mg/ml in PBS) was added to each well 4 hours prior to experiment termination in a 37°C incubator containing 5% CO_2 , the absorbance at 490 nm was read on a microplate reader (Thermo, USA). The IC_{50} values of the compounds for cytotoxicity were calculated by GraphPad Prism 6.0 software (GraphPad software, San Diego, CA, USA) from the dose-response curves.

4.4 Duration of the MDR reversal

The experiment was carried out as the reported procedures with minor modification.[33] In brief, K562/A02 cells were seeded in 96-well micro-titer plates

at 1×10^4 per well during logarithmic growth phase, cells were incubated for 24 h with or without 5.0 μM of **VRP**, **Tar**, **I-5** or PBS before being washed 0 or 3 times with culture medium. Then, the cells were incubated for 0, 6, 12, or 24 h before the addition of varying concentrations of DOX or vehicle. The incubation was continued for 48 h prior to the MTT assay.

4.5 DOX intracellular accumulation

The reported procedures with minor modification was employed for the detection of accumulation of DOX [25]. K562 and K562/A02 cells were seeded into 24-well plates 1.5×10^4 per well. Different concentrations of VRP, Tar and I-5 (0.5 μM , 2.5 μM , 5.0 μM) were pre-incubated with cells for 60 min. Then 20 μM DOX was added into each well and incubated for 90 min, washed with ice-cold PBS for three times at 4°C. The fluorescence intensity of cells can be observed through fluorescence microscope. Afterwards the cells were disintegrated by Triton \times 100 liquid. The mean fluorescence intensity (MFI) of accumulation intracellular DOX was measured by fluorescence spectrophotometer. Data were expressed as means \pm SD of three independent experiments.

4.6 Rh123 efflux assay

K562 and K562/A02 cells were seeded into 24-well plates 1.5×10^4 per well and incubated with 5 μM Rh123 for 60 min before washing with ice-cold PBS for three times. Then the cells were incubated with or without 2.0 μM I-5 or 5.0 μM VRP for another 90 min. Afterwards the cells were washed thrice in ice-cold PBS. Afterwards the cells were disintegrated by Triton \times 100 liquid [35]. The MFI of retained intracellular Rh123 was estimated by BD FACSCalibur flow cytometer through the FL1 tunnel. Data were expressed as means \pm SD of three independent experiments.

4.7 Western blotting

After 48h incubation with VRP (5.0 μM), **Tar** (5.0 μM), **I-5** (0.5 μM , 5.0 μM), K562/A02 cells were harvested and washed thrice with ice-cold PBS and lysed with RIPA lysis buffer containing 10% PMSF. Total protein was extracted by centrifuging at 12000r for 15 min at 4°C. Total protein content was determined by BCA Protein Assay kit. The Protein samples were separated by 8% SDS-PAGE gel electrophoresis

and the proteins were transferred to PVDF membranes. Then the membranes were blocked with TBST(10mM Tris-HCl, pH 7.5, 150mM NaCl and 0.1% Tween 20) containing 5% nonfat dried milk for 1h and probed with the specific P-gp antibody, β -tubulin antibody overnight at 4°C . After being washed with TBST 3 times, the membranes were incubated with the secondary antibodies for 2h at room temperature. After washing for another three times, proteins were visualized using the enhanced chemiluminescence detection system and Quantity One software were used to analyses the protein's band intensity [35, 36].

Acknowledgements

This study was supported by National Natural Science Foundation of China (No. 81872733, 81872734 and 81803353).

Conflict of interest

The authors declare no competing financial interest.

Reference

- [1] Mcguire S. World Cancer Report 2014. Geneva, Switzerland: World Health Organization, International Agency for Research on Cancer. *Adv. Nutr.* 2016; 7: 418-419.
- [2] Luqmani YA. Mechanisms of drug resistance in cancer chemotherapy. *Med. Princ. Pract.* 2014; 14: 35-48.
- [3] Housman G, Byler S, Heerboth S, et al. Drug Resistance in Cancer: An Overview. *Cancers (Basel)*. 2014; 6: 1769-1792.
- [4] Du B, Shim JS. Targeting Epithelial-Mesenchymal Transition (EMT) to Overcome Drug Resistance in Cancer. *Molecules*. 2016; 21: 965.
- [5] Reed JC, Miyashita T, Takayama S, et al. BCL-2 family proteins: regulators of cell death involved in the pathogenesis of cancer and resistance to therapy. *J. Cell. Biochem.* 2015; 60: 23-32.
- [6] Seguin L, Desgrosellier JS, Weis SM, et al. Integrins and cancer: regulators of cancer stemness, metastasis, and drug resistance. *Trends Cell Biol.* 2015; 25: 234-240.
- [7] Adorno-Cruz V, Kibria G, Liu X, et al. Cancer stem cells: targeting the roots of cancer, seeds of metastasis, and sources of therapy resistance. *Cancer Res.* 2015; 75: 924-929.
- [8] Dlugosz A, Janecka A. ABC Transporters in the Development of Multidrug Resistance in Cancer Therapy. *Curr. Pharm. Des.* 2016; 22: 4705-4716
- [9] Leslie EM, Deeley RG, Cole SP. Multidrug resistance proteins: role of P-glycoprotein, MRP1, MRP2, and BCRP (ABCG2) in tissue defense. *Toxicol. Appl. Pharmacol.* 2005; 204: 216-237.
- [10] And JA, Ling VJ. The Biochemistry of P-Glycoprotein-Mediated Multidrug Resistance. *Annu.*

Rev. Biochem. 1989; 58: 137-171.

[11] Binkhathlan Z, Lavasanifar AT. P-glycoprotein Inhibition as a Therapeutic Approach for Overcoming Multidrug Resistance in Cancer: Current Status and Future Perspectives. *Curr. Cancer Drug Targets.* 2013; 13: 326-346.

[12] Nobili S, Landini I, Mazzei T, et al. Overcoming tumor multidrug resistance using drugs able to evade P-glycoprotein or to exploit its expression. *Med. Res. Rev.* 2012; 32: 1220-1262.

[13] Tsuruo T, Iida H, Tsukagoshi S, et al. Overcoming of vincristine resistance in P388 leukemia in vivo and in vitro through enhanced cytotoxicity of vincristine and vinblastine by verapamil. *Cancer Res.* 1981; 41: 1967-1972.

[14] Pinto MM, Vasconcelos MH, Sousa E, et al. Three Decades of P-gp Inhibitors: Skimming Through Several Generations and Scaffolds. *Curr. Med. Chem.* 2012; 19: 1946-2025.

[15] Abdallah HM, Alabd AM, Eldine RS, et al. P-glycoprotein inhibitors of natural origin as potential tumor chemo-sensitizers: A review. *J. Adv. Res.* 2015; 6: 45-62.

[16] Palmeira A, Sousa E, Vasconcelos M, et al. Structure and Ligand-based Design of P-glycoprotein Inhibitors: A Historical Perspective. *Curr. Pharm. Des.* 2012; 18: 4197-4214.

[17] Joshi P, Vishwakarma RA, Bharate SC. Natural alkaloids as P-gp inhibitors for multidrug resistance reversal in cancer. *J. Med. Chem.* 2017; 138: 273-292.

[18] Nesi G, Colabufo NA, Contino M, et al. SAR study on arylmethoxyphenyl scaffold: looking for a P-gp nanomolar affinity. *Eur. J. Med. Chem.* 2014; 76: 558-566.

[19] Jekerle V, Klinkhammer W, Scollard DA, et al. In vitro and in vivo evaluation of WK-X-34, a novel inhibitor of P-glycoprotein and BCRP, using radio imaging techniques. *Int. J. Cancer.* 2010; 119: 414-422.

[20] Fox E, Bates S. Tariquidar (XR9576): a P-glycoprotein drug efflux pump inhibitor. *Anticancer. Ther.* 2007; 7: 447-459.

[21] Kwak JO, Lee SH, Lee GS, et al. Selective inhibition of MDR1 (ABCB1) by HM30181 increases oral bioavailability and therapeutic efficacy of paclitaxel. *Eur. J. Pharmacol.* 2010; 627: 92-98.

[22] Dheer D, Singh V, Shankar R. Medicinal attributes of 1,2,3-triazoles: Current developments. *Bioorg. Chem.* 2017; 71: 30-54.

[23] Kommi DN, Jadhavar PS, Kumar D, et al. "All-water" one-pot diverse synthesis of 1, 2-disubstituted benzimidazoles: hydrogen bond driven 'synergistic electrophile-nucleophile dual activation' by water. *Green Chem.* 2013; 15: 798-810.

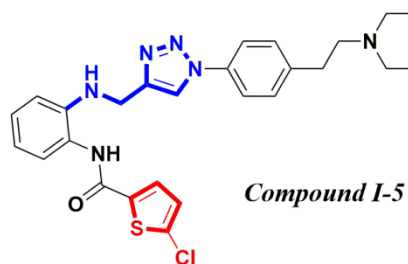
[24] Aichhorn S, Himmelsbach M, Schöfberger W. Synthesis of quinoxalines or quinolin-8-amines from N-propargyl aniline derivatives employing tin and indium chlorides. *Org. Biomol. Chem.* 2015; 13: 9373-9380.

[25] Liu B, Qiu Q, Zhao T, et al. Discovery of novel P-glycoprotein-mediated multidrug resistance inhibitors bearing triazole core via click chemistry, *Chem. Biol. Drug Des.* 2014; 84: 182-191.

[26] Jiao L, Qiu Q, Liu B, et al. Design, synthesis and evaluation of novel triazole core based P-glycoprotein-mediated multidrug resistance reversal agents. *Bioorg. Med. Chem.* 2014; 22: 6857-

6866.

- [27] Kang Y, Perry RR. Effect of alpha-interferon on P-glycoprotein expression and function and on verapamil modulation of doxorubicin resistance. *Cancer Res.* 1994; 54: 2952-2958.
- [28] Gao Y, Shi W, Cui J, et al. Design, synthesis and biological evaluation of novel tetrahydroisoquinoline derivatives as P-glycoprotein-mediated multidrug resistance inhibitors. *Bioorg. Med. Chem.* 2018; 26: 2420-2427.
- [29] Ghaleb H, Li H, Kairuki M, et al. Design, Design, Synthesis and Evaluation of a Novel Series of Inhibitors Reversing P-Glycoprotein-Mediated Multidrug Resistance. *Chem. Biol. Drug Des.* 2018; 92:1708-1716.
- [30] Jabbar S, Twentyman PR, Watson JV. The MTT assay underestimates the growth inhibitory effects of interferons. *Br. J. Cancer.* 1989; 60: 523-528.
- [31] Fu LW, Zhang YM, Liang YJ, et al. The multidrug resistance of tumour cells was reversed by tetrandrine in vitro and in xenografts derived from human breast adenocarcinoma MCF-7/adr cells. *Eur. J. Cancer.* 2002; 38: 418-426.
- [32] Wang N, Zhao L, Wu L, et al. Mechanistic Analysis of Taxol-induced Multidrug Resistance in an Ovarian Cancer Cell Line. *Asian Pac J Cancer Prev.* 2013; 14: 4983-4988.
- [33] Wong IL, Chan KF, Tsang KH, et al. Modulation of multidrug resistance protein 1 (MRP1/ABCC1)-mediated multidrug resistance by bivalent apigenin homodimers and their derivatives. *J. Med. Chem.* 2009; 52: 5311-5322.
- [34] Twentyman PR, Rhodes T, Rayner S. A comparison of rhodamine 123 accumulation and efflux in cells with P-glycoprotein-mediated and MRP-associated multidrug resistance phenotypes. *Eur. J. Cancer.* 1994; 30A: 1360-1369.
- [35] Wang YJ, Kathawala RJ, Zhang YK, et al. Motesanib (AMG706), a potent multikinase inhibitor, antagonizes multidrug resistance by inhibiting the efflux activity of the ABCB1. *Biochem. Pharmacol.* 2014; 90: 367-378.
- [36] Mudududdla R, Guru SK, Wani A, et al. 3-(Benzo[d][1,3]dioxol-5-ylamino)-N-(4-fluorophenyl)thiophene-2-carboxamide overcomes cancer chemoresistance via inhibition of angiogenesis and P-glycoprotein efflux pump activity. *Org. Biomol. Chem.* 2015; 13: 4296-4309.



- ◆ High potency, $EC_{50} = 46.83 \pm 4.6$ nM
- ◆ Long activity duration, > 24h
- ◆ Great increase of DOX cellular accumulation
- ◆ Suppress P-gp function
- ◆ No effect on P-gp expression

